Electronic Supplementary Information for

# Synthesis and Properties of a Rod-*g*-Rod Bottlebrush with a Semirigid Mesogen-Jacketed Polymer as the Side Chain

Hai-Jian Tian, Wei Qu, Yu-Feng Zhu, Zhihao Shen,* and Xing-He Fan*

Beijing National Laboratory for Molecular Sciences, Key Laboratory of Polymer Chemistry and Physics of Ministry of Education, College of Chemistry and Molecular Engineering, Peking University,
Beijing 100871, China

* To whom the correspondence should be addressed. E-mail: fanxh@pku.edu.cn; zshen@pku.edu.cn.

## Contents

1. Synthesis of the backbone and side chains S2
   1.1. Synthesis of azide-substituted poly(L-glutamate) S2
   1.2. Synthesis of α-alkyne-PMPCS S4
2. Characterization of the chemical structures of the bottlebrushes S5
3. SAXS analysis S7
   3.1. Model-independent methods S7
   3.2. Model-dependent methods S8
      3.2.1. Cylinder model S8
      3.2.2. Ellipsoid model S9
      3.2.3. Wormlike chain model S11
References S12

## 1. Synthesis of the backbone and side chains

### 1.1. Synthesis of azide-substituted poly(L-glutamate)

#### 1.1.1. Synthesis of γ-chloropropanyl-L-glutamate (2)

Chlorotrimethylsilane (10.5 mL, 83.0 mmol) was added to the mixture of L-glutamic acid (11.0 g, 75.0 mmol) and 3-chloropropanol (100 mL) via a syringe. The resulting suspension was stirred at ambient temperature for 2 days. The undissolved L-glutamic acid was removed by filtration. Addition of diethyl ether (500 mL) to the filtrate yielded a white solid which was collected by filtration. Further purification by recrystallization in ethanol/diethyl ether (1:3, v:v) afforded the final product as a white solid (9.2 g, 55% yield). $^1$H NMR (400 MHz, $D_2O$, $\delta$, ppm): 4.19 (t, 2H, $ClCH_2CH_2CH_2O$-), 4.00 (t, 1H, $CHNH_2$), 3.60 (t, 2H, $ClCH_2CH_2CH_2$-), 2.56 (t, 2H, -$COCH_2CH_2$-), 2.09–2.21 (m, 2H, -$COCH_2CH_2$-), 2.02 (p, 2H, $ClCH_2CH_2CH_2$-).

#### 1.1.2. Synthesis of γ-3-chloropropanyl-L-glutamate based *N*-carboxyanhydride (3)

Compound **2** (5.00 g, 22.5 mmol) and triphosgene (4.00 g, 13.5 mmol) were dissolved in anhydrous THF (100 mL) under nitrogen. The mixture was then immerged into an oil bath thermostated at 80 °C for about 0.5 h until the suspension became homogeneous. The solvent was removed under vacuum. The resulting liquid was then dissolved in ethyl acetate (80.0 mL) and washed with a cold saturated $NaHCO_3/H_2O$ solution. The organic layer was separated and dried over anhydrous $MgSO_4$ at 0 °C. Evaporation of the solvent yielded an oily liquid. Further purification by recrystallization in $CH_2Cl_2$/hexane at −85 °C in a deep freezer afforded the final product as a white solid (3.75 g, 67% yield). $^1$H NMR (400 MHz, $CDCl_3$, $\delta$, ppm): 6.81 (s, 1H, N*H*), 4.45 (t, 1H, C*H*NH), 4.27 (t, 2H, $ClCH_2CH_2CH_2O$-), 3.63 (t, 2H, $ClCH_2CH_2CH_2$-), 2.58 (t, 2H, -$COCH_2CH_2$-), 2.06–2.32 (m, 2H, -$COCH_2CH_2$-), 2.12 (t, 2H, $ClCH_2CH_2CH_2$-).

### 1.1.3. Synthesis of poly(γ-3-chloropropanyl-L-glutamate) (4, PCPLG)

A typical polymerization of **3** is described as follows. Compound **3** (1.00 g, 4.00 mmol) was dissolved in DMF (5.0 mL) in a Schlenk flask under nitrogen. After degassing by three freeze-pump-thaw cycles, a measured volume of HMDS (8.30 μL, 40.0 μmol) was subsequently added with a syringe. The reaction mixture was stirred at ambient temperature for 3 days and quenched by exposure to air. The raw product was precipitated in methanol. Further purification was done by dissolution in $CH_2Cl_2$ and precipitation from methanol. The resulting polymer was collected by filtration and dried under vacuum at 60 °C for 24 h (0.67 g, 81% yield). $^1$H NMR (400 MHz, $CDCl_3$, $\delta$, ppm): 7.90 (d, 1H, N*H*), 4.66 (s, 1H, C*H*NH), 4.31 (t, 2H, $ClCH_2CH_2CH_2O$-), 3.59 (t, 2H, $ClCH_2CH_2CH_2$-), 2.57 (br s, 2H, -$COCH_2CH_2$-), 1.96–2.26 (m, 2H, -$COCH_2CH_2$-), 2.11 (t, 2H, $ClCH_2CH_2CH_2$-).

### 1.1.4. Synthesis of poly(γ-3-azidopropanyl-L-glutamate) (5, PAPLG)

Polymer **4** (1.00 g, 4.90 mmol) and sodium azide (3.0 g, 46 mmol) were mixed in DMF (50.0 mL) and stirred at 60 °C for 2 days. The reaction mixture was then cooled to ambient temperature and passed through a neutral alumina column to remove any inorganic salts. The raw product was precipitated in methanol. Further purification was conducted by dissolution in $CH_2Cl_2$ and precipitation from methanol. The resulting polymer was collected by filtration and dried under vacuum at 60 °C (0.68 g, 70% yield). $^1$H NMR (400 MHz, $CDCl_3$, $\delta$, ppm): 7.88 (d, 1H, N*H*), 4.63 (s, 1H, C*H*NH), 4.24 (t, 2H, $ClCH_2CH_2CH_2O$-), 3.43 (t, 2H, $N_3CH_2CH_2CH_2$-), 2.56 (br s, 2H, -$COCH_2CH_2$-), 1.90–2.25 (m, 2H, -$COCH_2CH_2$-), 1.97 (t, 2H, $ClCH_2CH_2CH_2$-).

## 1.2. Synthesis of α-alkyne PMPCS

### 1.2.1. Synthesis of monomer {2,5-bis[(4-methoxyphenyl)oxycarbonyl]styrene} (MPCS)

MPCS was synthesized from 2,5-dimethylbenzonic acid and *p*-methyloxy phenol by the method described in literature.[1]

### 1.2.2. Synthesis of propargyl bromoisobutyrate-bromoisobutyrate (6)

Propargyl alcohol (5.50 g, 100 mmol) and triethylamine (25.0 mL) were dissolved in anhydrous THF (100 mL), and the solution was cooled down to 0 °C. A solution of 2-bromo-2-methylpropionyl bromide (15.0 g, 120 mmol) in THF (50.0 mL) was added dropwise. The reaction mixture was stirred at 0 °C for 30 min and then at ambient temperature overnight. The undissolved inorganic salts were removed by filtration. After removal of the solvent by evaporation, the solid obtained was dissolved in $CH_2Cl_2$ (50 mL) and further washed with water three times. The organic layer was separated and dried over anhydrous $MgSO_4$. Evaporation of the solvent under vacuum gave a yellow liquid, which was further purified by silica column chromatography to yield a colorless liquid (75% yield). $^1$H NMR (400 MHz, $CDCl_3$, $\delta$, ppm): 4.78 (d, 2H, C*H*$_2$O), 2.53 (t, 1H,C≡C*H*), and 1.96 (s, 6H, (C*H*$_3$)$_2$C).

### 1.2.3. Synthesis of α-alkyne PMPCS (7, PMPCS)

A typical polymerization of MPCS is as follows. MPCS (2.00 g, 0.500 mmol), compound **6** (2.00 mg, 10.0 μmol), CuBr (1.43 mg, 10.0 μmol), PMDETA (1.73 mg, 10.0 μmol), and chlorobenzene (10.0 mL) were introduced into a Schlenk flask under nitrogen. The Schlenk flask was degassed by three freeze-pump-thaw cycles, sealed under vacuum, and then immerged into an oil bath thermostated at 80 °C for 6 h. After that, the solution was quenched in cold water and passed through a neutral alumina column to remove the Cu(I) catalyst. The polymer was precipitated in methanol to obtain a white solid (70% yield).

## 2. Characterization of the chemical structures of the bottlebrushes

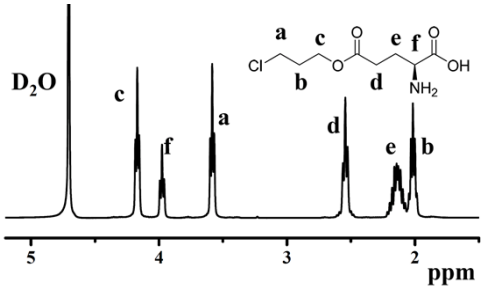


Fig. S1 $^{1}$H NMR spectrum of γ-chloropropanyl-L-glutamate.

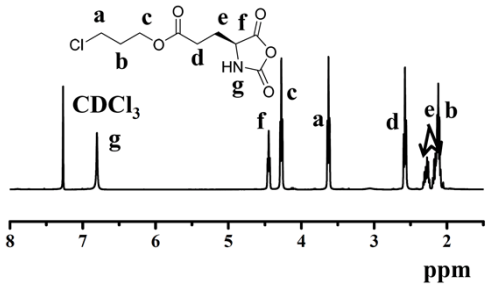


Fig. S2 $^{1}$H NMR spectrum of the *N*-carboxyanhydride based on γ-3-chloropropanyl-L-glutamate.

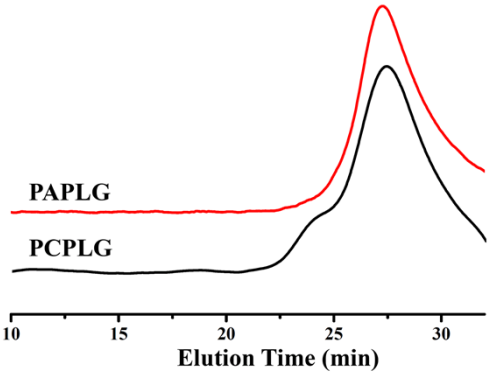


Fig. S3 Representative GPC traces of PCPLG ($M_w$ = 25.9×10$^3$ g mol$^{-1}$, PDI = 1.04) and the corresponding PAPLG.

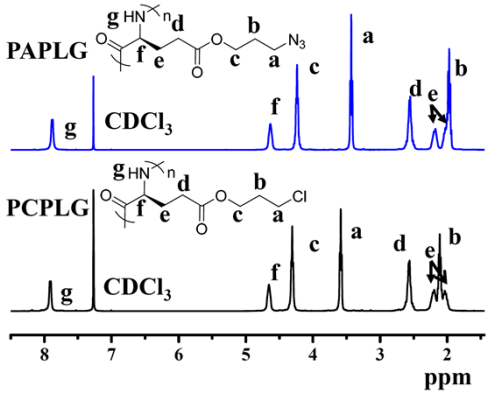


Fig. S4 $^{1}$H NMR spectra of PCPLG and PAPLG in $CDCl_3/CF_3CO_2D$ (v:v = 75:25).

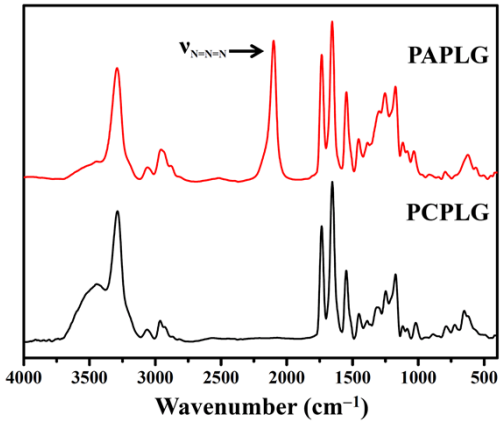


Fig. S5 FT-IR spectra of PCPLG and PAPLG in the solid state.

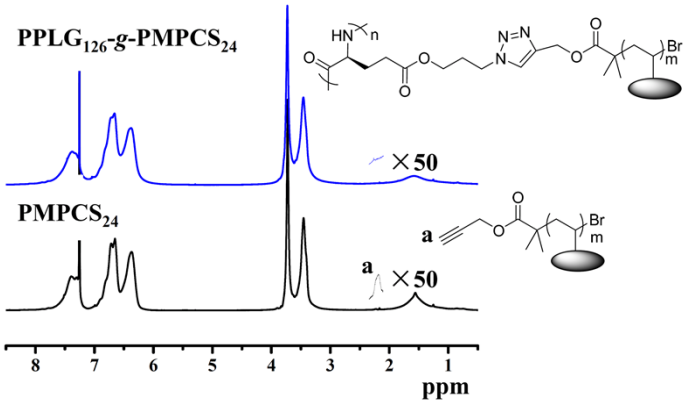


Fig. S6 Representative $^{1}$H NMR spectra of $PMPCS_{24}$ and the corresponding $PPLG_{126}$-*g*-$PMPCS_{24}$.

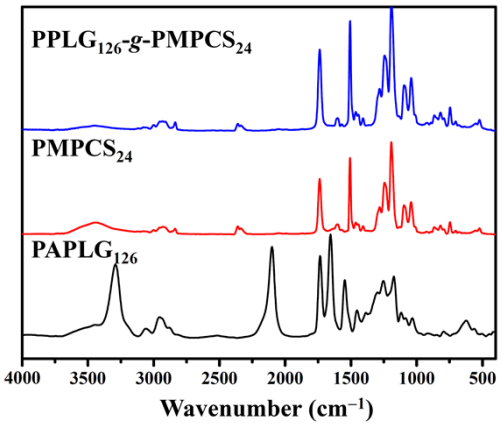


Fig. S7 FT-IR spectra of $PAPLG_{126}$, $PMPCS_{24}$, and $PPLG_{126}$-*g*-$PMPCS_{24}$ in the solid state.

## 3. SAXS analysis

### 3.1. Model-independent methods

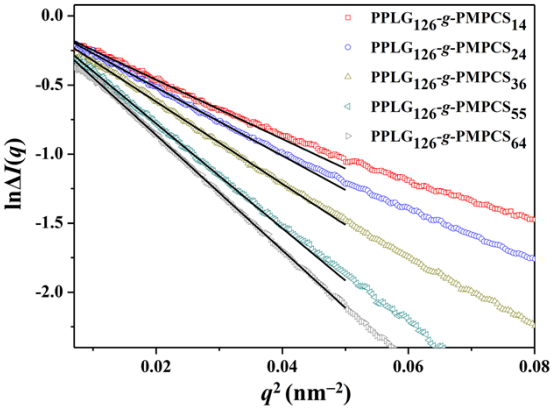


Fig. S8 Guinier plots of $\ln\Delta I(q)$ as a function of $q^2$ for PPLG-*g*-PMPCS bottlebrushes in THF at 25 °C.

Table S1. Calculated Results of the Bottlebrushes by the IFT Method

| Bottlebrush | $D_{max}$ (nm) | $R_{g,IFT}$ (nm) |
|---|---|---|
| $PPLG_{126}$-*g*-$PMPCS_{14}$ | 34 | 8.47 |
| $PPLG_{126}$-*g*-$PMPCS_{24}$ | 33 | 9.04 |
| $PPLG_{126}$-*g*-$PMPCS_{36}$ | 33 | 9.76 |
| $PPLG_{126}$-*g*-$PMPCS_{55}$ | 35 | 10.71 |
| $PPLG_{126}$-*g*-$PMPCS_{64}$ | 36 | 11.07 |

### 3.2. Model-dependent methods

#### 3.2.1. Cylinder model

The cylindrical particle form factor is described by two parameters: *R*, radius of the cylinder and *L*, length of the cylinder.[2] The resulting fits to the data are shown in Figure S9 and Table S2.

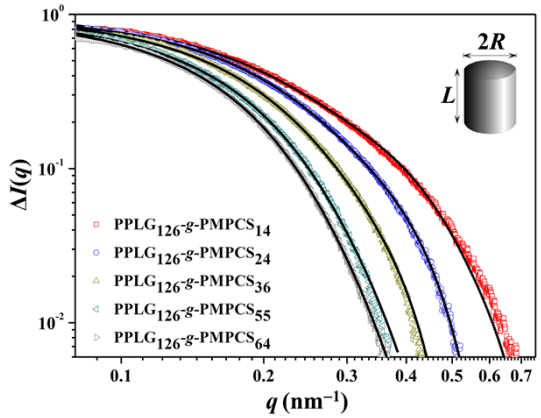


Fig. S9 Fitting results based on the cylinder model for the bottlebrushes with side chains of different DPs. The upper right corner illustrates the two parameters in the cylinder model.

Table S2. Fitting Results of the Bottlebrushes from the Cylinder Model

| **Bottlebrush** | $R$ **(nm)** [a] | $L$ **(nm)** [b] | $R_{g,cyl}$ **(nm)** [c] |
|---|---|---|---|
| $PPLG_{126}$-*g*-$PMPCS_{14}$ | 5.10 | 26.6 | 8.48 |
| $PPLG_{126}$-*g*-$PMPCS_{24}$ | 6.46 | 25.6 | 8.69 |
| $PPLG_{126}$-*g*-$PMPCS_{36}$ | 7.88 | 26.7 | 9.51 |
| $PPLG_{126}$-*g*-$PMPCS_{55}$ | 9.34 | 27.6 | 10.35 |
| $PPLG_{126}$-*g*-$PMPCS_{64}$ | 9.96 | 29.2 | 10.98 |

[a] Cross-sectional radius of the cylinder.

[b] Length of the cylinder.

[c] From the derived parameters $R$ and $L$, the radius of gyration ($R_{g,cyl}$) can be calculated by $R_{g,cyl}^2 = \frac{R^2}{2} + \frac{L^2}{12}$.

### 3.2.2. Ellipsoid model

A three-dimensional ellipsoid can be obtained by rotating an ellipse around one of its principal axes. The ellipsoidal particle form factor is described by two parameters: $R$, radius of the rotational axis and $v$, the ratio of the radius of the semi-principle axis to that of the equatorial axis.[3] The resulting fits to the data are shown in Figure S10 and Table S3.

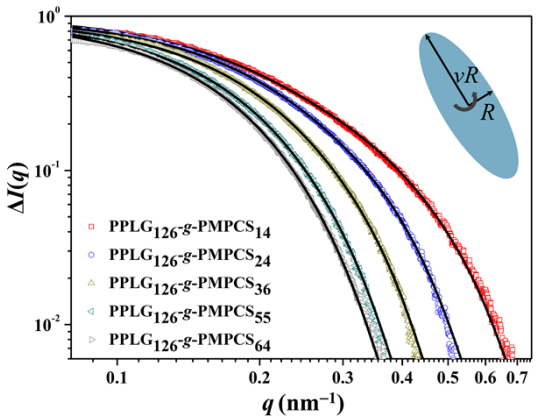


Fig. S10 Fitting results based on the ellipsoid model for the bottlebrushes with side chains of different DPs. The upper right corner illustrates the two parameters in the ellipsoid model.

Table S3. Fitting Results of the Bottlebrushes from the Ellipsoid Model

| **Bottlebrush** | $R$ **(nm)** [a] | $v$ [b] | $a_s$ [c] | $R_{g,ell}$ **(nm)** [d] |
|---|---|---|---|---|
| PPLG$_{126}$-*g*-PMPCS$_{14}$ | 5.34 | 3.45 | 0.61 | 8.90 |
| PPLG$_{126}$-*g*-PMPCS$_{24}$ | 6.85 | 2.57 | 0.42 | 8.99 |
| PPLG$_{126}$-*g*-PMPCS$_{36}$ | 8.41 | 2.14 | 0.30 | 9.65 |
| PPLG$_{126}$-*g*-PMPCS$_{55}$ | 9.93 | 1.93 | 0.23 | 10.63 |
| PPLG$_{126}$-*g*-PMPCS$_{64}$ | 10.62 | 1.89 | 0.21 | 11.19 |

[a] Radius of the rotational axis.

[b] The ratio of the radius of the semi-principle axis to that of the equatorial axis.

[c] Asphericity parameter, which can be determined using $a_s = 1 - 3\frac{1+2v^2}{\left(2+v^2\right)^2}$.[4]

[d] From the derived parameters $R$ and $v$, the radius of gyration ($R_{g,ell}$) can be calculated by $R_{g,ell}^2 = \frac{2R^2 + (vR)^2}{5}$.[5]

### 3.2.3. Wormlike chain model

The wormlike chain (WLC) model is often used to describe a flexible cylinder, such as some wormlike micelles and bottlebrush polymers. The model used here was developed by Kholodenko,[6] and it is described by three parameters: $R$, cross-sectional radius, $l_p$, persistence length, and $L_c$, contour length.[7] In this work, as the backbone DP is fixed at 126, we set $L_c$ to a fixed value of 0.36×126 nm = 45 nm as the length of the backbone. The resulting fits to the data are shown in Figure S11 and Table S4.

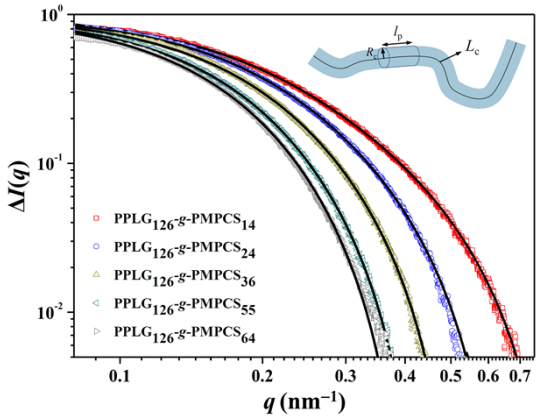


Fig. S11 Fitting results based on the WLC model for the bottlebrushes with side chains of different DPs. The upper right corner illustrates the two parameters in the WLC model.

Table S4. Fitting Results of the Bottlebrushes from the WLC Model

| **Bottlebrush** | $R$ **(nm)** [a] | $l_p$ **(nm)** [b] | $R_{g,m}$ **(nm)** [c] | $R_{g,WLC}$ **(nm)** [d] |
|---|---|---|---|---|
| $PPLG_{126}$-*g*-$PMPCS_{14}$ | 4.41 | 5.2 | 7.52 | 8.43 |
| $PPLG_{126}$-*g*-$PMPCS_{24}$ | 5.82 | 4.8 | 7.30 | 8.87 |
| $PPLG_{126}$-*g*-$PMPCS_{36}$ | 7.27 | 5.0 | 7.41 | 9.72 |
| $PPLG_{126}$-*g*-$PMPCS_{55}$ | 8.70 | 5.7 | 7.76 | 10.81 |
| $PPLG_{126}$-*g*-$PMPCS_{64}$ | 9.30 | 6.4 | 8.06 | 11.40 |

[a] Cross-sectional radius.

[b] Persistence length.

[c] From the derived parameters $l_p$ and $L_c$, the radius of gyration of the main chain ($R_{g,m}$) can be calculated by $R_{g,m}^2 = \frac{L_c l_p}{3} - l_p^2 + \frac{2l_p^3}{L_c} - \frac{2l_p^4}{L_c^2}\left(1 - e^{-\frac{L_c}{l_p}}\right)$.[8,9]

[d] The radius of gyration is calculated from $R_{g,WLC}^2 = R_{g,m}^2 + \frac{3}{4}R^2$.[10]

## References


(1) Zhang, D.; Liu, Y. X.; Wan, X. H.; Zhou, Q. F. *Macromolecules* **1999**, *32*, 5183-5185.

(2) http://sasfit.ingobressler.net/manual/Cylinder.

(3) http://sasfit.ingobressler.net/manual/Ellipsoid.

(4) Gillissen, M. A. J.; Terashima, T.; Meijer, E. W.; Palmans, A. R. A.; Voets, I. K. *Macromolecules* **2013**, *46*, 4120-4125.

(5) Cheng, G.; Melnichenko, Y. B.; Wignall, G. D.; Hua, F.; Hong, K.; Mays, J. W. *Macromolecules* **2008**, *41*, 9831-9836.

(6) Kholodenko, A. L. *Macromolecules* **1993**, *26*, 4179-4183.

(7) http://sasfit.ingobressler.net/manual/KholodenkoWorm.

(8) Kikuchi, M.; Lien, L. T. N.; Narumi, A.; Jinbo, Y.; Izumi, Y.; Nagai, K.; Kawaguchi, S. *Macromolecules* **2008**, *41*, 6564-6572.

(9) Saito, Y.; Lien, L. T. N.; Jinbo, Y. J.; Kumaki, J.; Narumi, A.; Kawaguchi, S. *Polym. J.* **2013**, *45*, 193-201.

(10) Zhang, B.; Groehn, F.; Pedersen, J. S.; Fischer, K.; Schmidt, M. *Macromolecules* **2006**, *39*, 8440-8450.